

Hamiltonian analysis of the transition to the high-gain regime in a Compton free-electron-laser amplifier

D. Farina

Istituto di Fisica del Plasma, Consiglio Nazionale delle Ricerche, via Bassini 15, 20133 Milano, Italy

F. Casagrande, U. Colombo, and R. Pozzoli

Dipartimento di Fisica, Università di Milano, via Celoria 16, 20133 Milano, Italy

(Received 7 June 1993; revised manuscript received 1 November 1993)

The dynamics of a Compton free-electron-laser amplifier is described by a Hamiltonian treatment. The structure of the $2N$ -dimensional phase space, N being the number of electrons, and the stability of the critical points are investigated with the detuning as control parameter. It is shown that the small-gain and high-gain regimes are characterized by different phase-space topologies. In particular, the transition to the high-gain regime is described as a bifurcation in which two well-defined fixed points coalesce. To test the validity of this description, the period of the saturation oscillation of the radiation field amplitude is evaluated by means of the Lie-transform method.

PACS number(s): 41.60.Cr, 03.20.+i

I. INTRODUCTION

In a Compton free-electron-laser (FEL) amplifier, a low-density, highly relativistic electron beam, injected along the axis of a wiggler, can amplify a copropagating radiation field [1,2]. Under proper conditions, the electrons bunch on the scale of a radiation wavelength, and, starting from a negligible initial value, the field amplitude exhibits as a function of the wiggler length a lethargic stage followed by an exponential growth up to saturation, where nearly periodic large-amplitude oscillations set in. Here, we denote this overall behavior high-gain regime, in contrast to the small-gain regime where the electrons behave as almost free particles and the radiation field oscillates close to its initial value for any interaction length. In the analysis of the Compton FEL dynamics, a suitable control parameter is the (dimensionless) detuning δ of the initial average electron energy γ_0 from the resonance value γ_R . The linear stability analysis of the FEL equations around an initial (equilibrium) condition with a nearly unbunched, monoenergetic beam and no field excitation [3] shows the existence of an instability threshold at a well-defined critical δ value $\delta_C = (\frac{27}{4})^{1/3}$. From the numerical integration of the full FEL equations, it turns out that the high-gain regime develops from the linearly unstable regime characterized by δ values smaller than δ_C . The small-gain regime corresponds to the linearly stable regime at δ values larger than δ_C .

The dynamics of the system has been described by different theoretical approaches [4,5]. Here, we consider the Hamiltonian treatment of the Compton FEL [6]. In the Hamiltonian framework, one basic problem remained unsolved, i.e., no clear picture of the transition occurring in the behavior of the system at the critical detuning $\delta = \delta_C$ has yet been done. A preliminary result in this direction was obtained only for the limiting case of one degree of freedom [7]: the analysis of the one-electron

phase space shows a sharp change in the electron orbit topology, occurring just at the value $\delta = \delta_C$. The one-particle Hamiltonian relevant to this process is also found in the analysis of other physical phenomena and has been thoroughly analyzed in different contexts [8,9].

In this paper, we refer to the system of N electrons self-consistently coupled with the radiation field, described by a Hamiltonian with N degrees of freedom, and investigate the topological changes of the phase-space structure at varying δ . We show that (in analogy with the one-particle case) the transition from the small- to the high-gain regime is connected to a bifurcation in the $2N$ -dimensional phase space, where the only hyperbolic point present in the system disappears, and the dynamics is determined by the presence of one elliptic point. This result is obtained by means of the stability analysis of the singular points, and is confirmed by direct numerical integration of the electron motion. To emphasize the role of the main singular points in each regime, a small dissipation is introduced in the system.

The Hamiltonian description of the system allows one to evaluate quantitatively some of its characteristics by means of well-developed analytical techniques. We consider here the computation of the (spatial) periodicity of nonlinear oscillations in the saturation regime, which is generally missed in the description by other theoretical models. The relevant analysis is performed by means of a canonical perturbation technique, the Lie-transform method [10]. The very good agreement of the obtained results with the numerical simulation may be taken as a confirmation of the validity of our approach.

The paper is organized as follows. In Sec. II the Hamiltonian description of FEL dynamics is introduced. Section III is devoted to the analysis of the phase space of the system. Section IV contains the explicit computation of the period of nonlinear oscillations in the high-gain regime. Concluding remarks are presented in Sec. V.

II. HAMILTONIAN MODEL OF A COMPTON FEL AMPLIFIER

A suitable starting point for the description of the dynamical regimes of a FEL is given by the evolution equations for the coupled system of N electrons with relativistic velocities in the z direction, and a copropagating quasimonochromatic, circularly polarized radiation field, interacting during the passage in a helical wiggler [11,12]. In compact dimensionless form the equations read [5]

$$\begin{aligned} \frac{d\theta_j}{d\bar{z}} &= P_j, \\ \frac{dP_j}{d\bar{z}} &= -[\tilde{A} \exp(i\theta_j) + \text{c.c.}], \\ \frac{d\tilde{A}}{d\bar{z}} &= \langle \exp(-i\theta) \rangle + i\delta \tilde{A}, \end{aligned} \quad (1)$$

with $j=1, \dots, N$. The symbol $\langle \rangle$ corresponds to averaging over the N particles. The j th electron is described by the variables θ_j, P_j , where $\theta = (k + k_0)z - \omega t - 2k_0\rho\delta z$ is the electron phase relative to the ponderomotive potential (radiation + wiggler), and $P_j = (1/\rho)(\gamma_j - \langle \gamma \rangle_0) / \langle \gamma \rangle_0$ is the relative energy variation, γ_j being the electron energy and $\langle \gamma \rangle_0$ the initial average value. The evolution of the system is given in terms of the dimensionless longitudinal coordinate $\bar{z} = 2k_0\rho z$. The field is described by the complex dimensionless vector potential $\tilde{A} \equiv |A| \exp(i\phi)$ with real amplitude $|A| = eE / [mc\omega_p(\rho\gamma_R)^{1/2}]$, where E is the rms electric field, $\omega_p = (4\pi e^2 n/m)^{1/2}$ is the plasma frequency, γ_R is the dimensionless resonant electron energy $\gamma_R = [k(1+a_0^2)/2k_0]^{1/2}$, $a_0 = eB_0/(k_0 mc^2)$ is the undulator parameter, and B_0 the rms wiggler field. Here, $\omega = kc$ is the central radiation frequency, k_0 is the wave number associated with the spatial wiggler periodicity, δ is the detuning parameter

$$\delta = \frac{1}{\rho} \frac{\langle \gamma \rangle_0 - \gamma_R}{\gamma_R},$$

and ρ is the FEL parameter

$$\rho = \frac{1}{\gamma_R} \left[\frac{a_0}{4} \frac{\omega_p}{k_0 c} \right]^{2/3}.$$

The main assumptions underlying Eqs. (1) are (i) one-dimensional dynamics; (ii) steady-state operation, i.e., negligible propagation effects during the interaction; (iii) slowly varying envelope approximation for the field evolution; (iv) Compton regime, typical of highly relativistic low-density electron beams.

The system (1) depends on a single dimensionless parameter δ . Moreover, it admits a constant of motion,

$$\langle P \rangle + |A|^2 = \text{const}, \quad (2)$$

which describes the energy conservation of the system, and rules the energy transfer between the electrons and the radiation field.

Equations (1) admit a stationary solution for an initial condition with a monoenergetic, unbunched beam, and

no field excitation:

$$P_{j0} = 0, \quad \langle \exp(-i\theta) \rangle_0 = 0, \quad \tilde{A}_0 = 0. \quad (3)$$

Linearizing Eqs. (1) around the equilibrium condition (3), it is found that the system is stable when $\delta > \delta_C$, and unstable when $\delta \leq \delta_C$, where the critical value of detuning parameter $\delta_C = (27/4)^{1/3}$ is the instability threshold for exponential field amplification [3].

The system (1) can be written in a Hamiltonian formalism. Actually, taking into account the constant of motion (2), we can introduce the following autonomous Hamiltonian function dependent on $2N$ variables q_j, p_j , ($j=1, \dots, N$):

$$\begin{aligned} H(q_1, \dots, q_N; p_1, \dots, p_N) &= \frac{1}{2} \sum_{j=1}^N p_j^2 + 2[\Delta - \langle p \rangle]^{1/2} \\ &\quad \times \sum_{j=1}^N \sin q_j, \end{aligned} \quad (4)$$

where

$$q_j = \theta_j + \phi, \quad p_j = P_j + \delta, \quad (5)$$

and

$$\Delta = \delta + |A|_0^2. \quad (6)$$

Hamilton's equations of motion are

$$\begin{aligned} \dot{q}_j &= \frac{\partial H}{\partial p_j} = p_j - \frac{\langle \sin q \rangle}{\sqrt{\Delta - \langle p \rangle}}, \\ \dot{p}_j &= -\frac{\partial H}{\partial q_j} = -2\sqrt{\Delta - \langle p \rangle} \cos q_j \end{aligned} \quad (7)$$

for $j=1, \dots, N$, where dots mean differentiation with respect to the variable \bar{z} , and the initial momentum condition now reads $\langle p \rangle_0 = \delta$.

Note that the field variables $|A|$ and ϕ do not enter explicitly in Eq. (4), and can be obtained by means of Eq. (2), $|A|^2 = \Delta - \langle p \rangle$, and by the equation $\dot{\phi} = \dot{q}_j + \delta - p_j$. Then, the Hamiltonian (4) depends on the only parameter Δ , which represents the total energy of the system. It describes a system of N pendulums coupled by the consistent field, which depends only on the average $\langle p \rangle$. This Hamiltonian function will be the basis of the subsequent analysis of the FEL dynamics.

Hamilton's equations have been solved numerically for a representative set of particles with initial conditions corresponding to a weak electric field, and an unbunched monoenergetic electron beam, i.e., conditions close to Eqs. (3): $p_{j0} = \delta$, $|A|_0 \ll 1$, and uniform phase distribution (in the following we refer to initial conditions of this kind). The behaviors of the squared field amplitude $|A|^2$ and of the average quantity $\langle \sin q \rangle$, which describes the phase bunching of the electrons, as a function of \bar{z} have been analyzed both in the stable and unstable regime. When $\delta > \delta_C$ (stable case), the system evolves, remaining always close to the initial condition (3). The energy of the particles does not vary appreciably, and a nearly unbunched electron beam remains unbunched (Fig. 1). When $\delta \leq \delta_C$ (unstable case), the scenario is completely

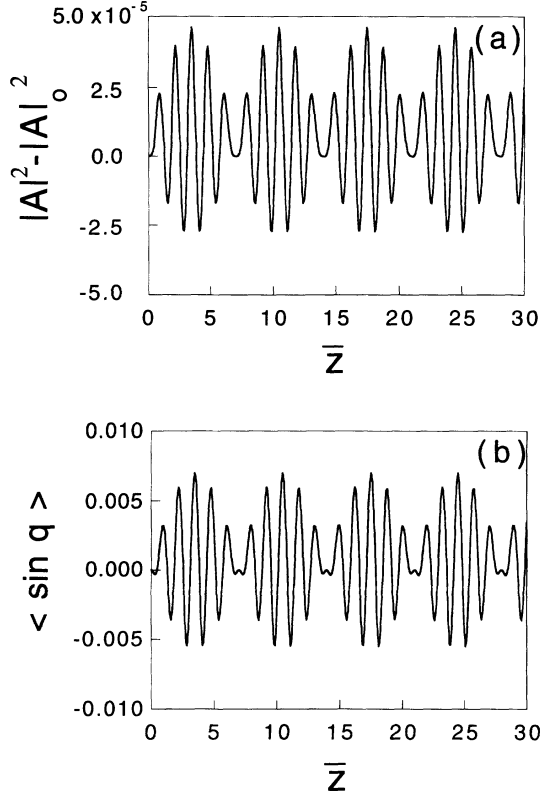


FIG. 1. Small-gain regime: behavior of the dimensionless squared field amplitude: $|A|^2 = \Delta - \langle p \rangle$ (a), and of $\langle \sin q \rangle$ (b) as a function of the longitudinal dimensionless coordinate \bar{z} . The parameters are $\delta = 5$, and $|A|_0^2 = 2 \times 10^{-4}$.

different, and cooperative effects show up. For large enough \bar{z} , both the field amplitude and the electron bunching parameter exhibit an exponential growth up to a peak value, followed by a nearly periodic regime (Fig. 2).

III. PHASE-SPACE ANALYSIS

To explore the relationship between the different FEL regimes and the relevant phase-space structure, the phase-space topology of the Hamiltonian (4) has been investigated considering the stability of the fixed points, which are the stationary solutions of the system (7), i.e., of the following system of $2N$ equations dependent on the parameter Δ :

$$p_j - \frac{\langle \sin q \rangle}{\sqrt{\Delta - \langle p \rangle}} = 0, \quad (8a)$$

$$2\sqrt{\Delta - \langle p \rangle} \cos q_j = 0, \quad (8b)$$

with $j = 1, \dots, N$. The phase values of a fixed point \bar{q}_j are immediately obtained by Eqs. (8b), and read $\bar{q}_j = \pm\pi/2$. As can be seen from the investigation of Eqs. (8a), all the action values coincide, $p_j = \bar{p}_j = \bar{p}$, and are determined by the mean value $\alpha \equiv \langle \sin \bar{q} \rangle$, where $\alpha = (N - 2k)/N$, and k ($k = 0, 1, \dots, N$) is the number of \bar{q}_j 's corresponding to the angle $-\pi/2$, and $N - k$ to $\pi/2$. For given α and Δ ,

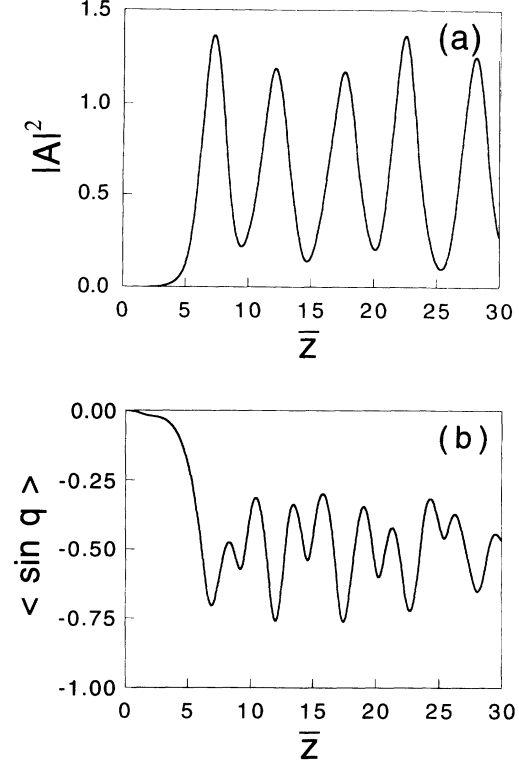


FIG. 2. High-gain regime: behavior of the dimensionless squared field amplitude $|A|^2$ (a), and of $\langle \sin q \rangle$ (b) as a function of the longitudinal dimensionless coordinate \bar{z} . The parameters are $\delta = 0$, and $|A|_0^2 = 2 \times 10^{-4}$.

the solutions of the system (8) can be expressed in terms of the roots of the cubic equation

$$\Lambda^3 - \Delta\Lambda + \alpha = 0, \quad (9)$$

where $\Lambda = \sqrt{\Delta - \bar{p}}$, with $\Lambda > 0$, and $|\alpha| \leq 1$. For $\Delta < 0$, Eq. (9) has one solution only for $\alpha \leq 0$. For $0 \leq \Delta \leq \Delta_C$, where $\Delta_C = (\frac{27}{4})^{1/3}$, the equation has one solution for $\alpha < 0$, two solutions for $0 < \alpha \leq (\Delta/\Delta_C)^{3/2}$, and no solutions for $(\Delta/\Delta_C)^{3/2} < \alpha \leq 1$. For $\Delta > \Delta_C$, there is still one solution for $\alpha \leq 0$, and two solutions for $\alpha > 0$. These results are summarized in Fig. 3, where the solutions of Eq. (9) are plotted versus α for different values of the parameter Δ .

Note that for given α - and Λ -value solutions of Eq. (9), there exist $\binom{N}{k}$ fixed points corresponding to the possible angle permutations. The only points which are unequivocally determined are those with all $\bar{q}_j = -\pi/2$ or $\pi/2$, and $\alpha = -1$ or $+1$, respectively. The two points with $\alpha = 1$ exist only for $\Delta > \Delta_C$, they merge together at $\Delta = \Delta_C$, and then disappear. The same behavior is found for positive Δ above the threshold value Δ_C at $\alpha = (\Delta/\Delta_C)^{3/2}$, so that the number of fixed points decreases with decreasing Δ . However, the bifurcation occurring at $\Delta = \Delta_C$ and $\alpha = 1$ seems to be the main one.

The linear stability of the fixed points of the Hamiltonian (4) can be investigated linearizing the equations of motion (7) around the singular points. Setting

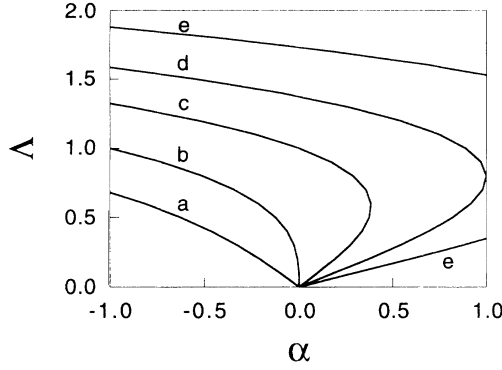


FIG. 3. Solutions of the cubic equation (9), for different Δ values. Λ and α characterize the fixed point coordinates, \bar{p} , \bar{q} , being $\Lambda = \sqrt{\Delta - \bar{p}}$, and $\alpha = \langle \sin \bar{q} \rangle$. The curves refer to the following cases: *a*, $\Delta < 0$; *b*, $\Delta = 0$; *c*, $0 < \Delta < \Delta_C$; *d*, $\Delta = \Delta_C$; *e*, $\Delta > \Delta_C$. The elliptic point corresponds to $\alpha = -1$. Curve *d* corresponds to the appearance of the hyperbolic point. In curve *e* the hyperbolic point corresponds to $\alpha = 1$ and to the largest value of Λ .

$q_j = \bar{q}_j + \delta q_j$, and $p_j = \bar{p}_j + \delta p_j$ ($j = 1, \dots, N$), the linearized system reads

$$\begin{aligned} \delta \dot{q}_j &= \delta p_j - \frac{\alpha}{2N\Lambda^3} \sum_{l=1}^N \delta p_l, \\ \delta \dot{p}_j &= \pm 2\Lambda \delta q_j, \end{aligned} \quad (10)$$

where the \pm sign corresponds to $\bar{q}_j = \pm \pi/2$. The linear stability of each fixed point can be determined by the eigenvalues λ of the linear operator defined by system (10) [13], which are solutions of the eigenequation

$$\begin{aligned} &(\lambda^2 - 2\Lambda)^{N-k-1} (\lambda^2 + 2\Lambda)^{k-1} \\ &\times \left[\lambda^4 + \frac{\alpha^2}{\Lambda^2} \lambda^2 - 4\Lambda^2 \left(1 - \frac{\alpha}{2\Lambda^3} \right) \right] = 0. \end{aligned} \quad (11)$$

The eigenvalues determined by the roots of the first two factors in Eq. (11) are always real and pure imaginary, respectively, independent of the values of Δ . With Δ varying, the main features of this dynamical system are described by the last factor in Eq. (11), which contains the coupling among the electrons due to the self-consistent field.

The most relevant cases are those with $\alpha = -1, +1$, which correspond to $k = N, 0$, respectively. For $\alpha = -1$, Eq. (11) reads

$$(\lambda^2 + 2\Lambda)^{N-1} \left[\lambda^2 + 2\Lambda + \frac{1}{\Lambda^2} \right] = 0. \quad (12)$$

All the roots of Eq. (12) are purely imaginary for any Δ value, and read $\lambda = \pm i\sqrt{2\Lambda + 1/\Lambda^2}$, and $\lambda = \pm i\sqrt{2\Lambda}$, multiple $N-1$. Thus the point corresponding to $\alpha = -1$ is elliptic. For $\alpha = 1$ (and $\Delta \geq \Delta_C$), Eq. (11) reads explicitly

$$(\lambda^2 - 2\Lambda)^{N-1} \left[\lambda^2 - 2\Lambda + \frac{1}{\Lambda^2} \right] = 0. \quad (13)$$

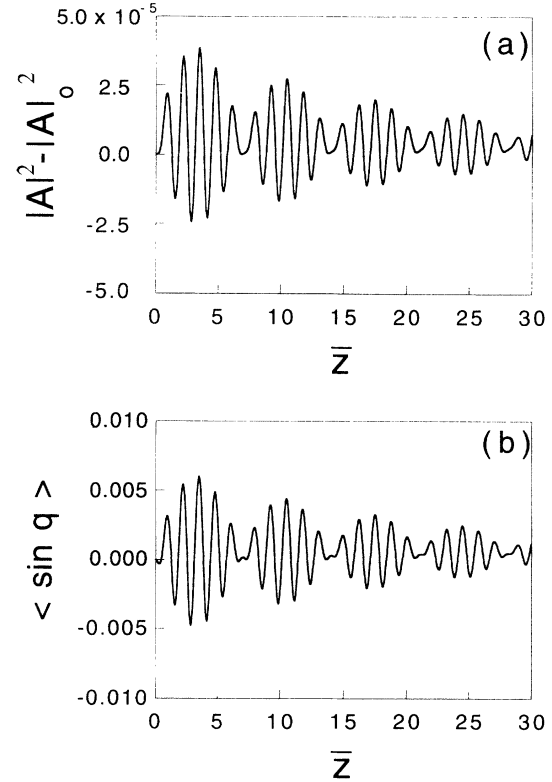


FIG. 4. Same as in Fig. 1, when a dissipative term is added to the equations of motion. The damping parameter η is equal to 0.1.

For $\Lambda > 2^{-1/3}$, all the eigenvalues are real: $\lambda = \pm\sqrt{2\Lambda - 1/\Lambda^2}$, and $\lambda = \pm\sqrt{2\Lambda}$, multiple $N-1$. The fixed point is hyperbolic and corresponds to the upper branch of Eq. (9). For $\Lambda < 2^{-1/3}$, i.e., on the lower branch of Eq. (9), there is an elliptic point only when $N=1$. For $N > 1$, there are $2N-2$ real eigenvalues $\lambda = \pm\sqrt{2\Lambda}$, and two imaginary eigenvalues $\lambda = \pm i\sqrt{1/\Lambda^2 - 2\Lambda}$, and the singular point is neither elliptic nor hyperbolic.

When $|\alpha| \neq 1$, some eigenvalues are real and some complex, and the corresponding singular points can never be stable. Moreover, we note that the last factor in Eq. (11) can be written

$$\left[\lambda^4 + \frac{\alpha^2}{\Lambda^2} \lambda^2 + 2 \frac{d\alpha}{d\Lambda} \right]. \quad (14)$$

Then, the coalescence of two critical points (occurring at $d\alpha/d\Lambda = 0$) implies the existence of the double root $\lambda = 0$.

Summarizing the obtained results, for $N > 1$ we find only a hyperbolic point for $\Delta \geq \Delta_C$ at $\alpha = 1$ and $\Lambda > 2^{-1/3}$, and an elliptic point at $\alpha = -1$, for any Δ value. It can be shown that this elliptic point is a minimum for the Hamiltonian (4).

We note that the critical Δ_C value coincides with the threshold value δ_C obtained in the stability analysis around a vanishingly small field amplitude, mentioned in Sec. II. From the above analysis of the phase space, we

can then conclude that in the small-gain FEL regime, the phase-space topology is governed by the presence of the (only) hyperbolic point. The transition to the high-gain regime corresponds to the occurrence of a bifurcation, and to the subsequent disappearance of the hyperbolic point. As a consequence, in the high-gain regime the system is strongly influenced by the presence of the elliptic point. Once the main topological modification of the phase space has occurred, subsequent bifurcations (at decreasing Δ) of nonpure hyperbolic fixed points introduce only minor changes in the behavior of the system.

To test the attractor properties of the elliptic point when the hyperbolic point disappears, we have investigated the case in which a term representing (formally) a dissipative process has been introduced in the system, adding the term $-\eta(p_j - p_{j0})$, with η positive and small, to the equation for the evolution of p_j in Eqs. (7). Note that the rate of contraction of phase-space volume is given by $N\eta$. The behavior of the system has been analyzed numerically in the same cases already presented in Figs. 1 and 2, relevant to the small- and high-gain regime, respectively. For $\Delta > \Delta_C$ (small gain), both the field amplitude and the bunching parameter perform damped oscillations around the initial values, with a frequency very close to that of the nondissipative case. For $\Delta < \Delta_C$ (high gain), $|A|^2(\bar{z})$ exhibits the same exponential increase as in the nondissipative case, and then performs damped oscillations around the value $\Lambda_e^2 \equiv \Delta - p_e$ (p_e being the

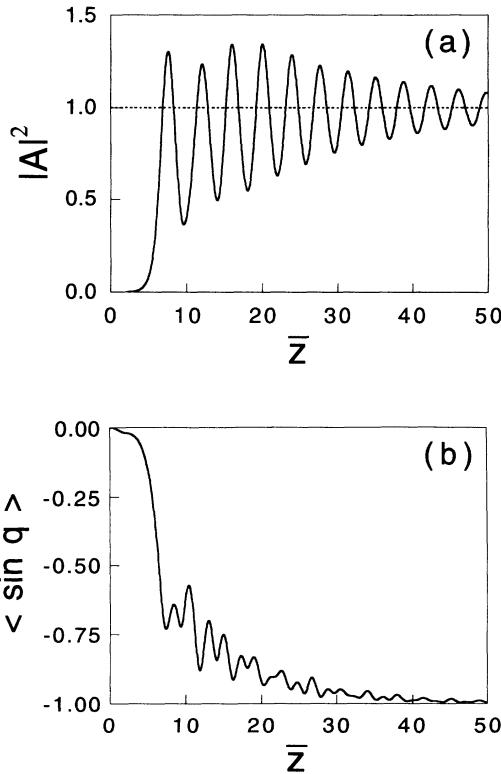


FIG. 5. Same as in Fig. 2, when a dissipative term is added to the equations of motion. The damping parameter η is equal to 0.1. The dotted line in (a) represents the squared field amplitude $|A|^2 = \Lambda_e^2 \equiv \Delta - p_e$, determined by the value of the elliptic point momentum p_e .

momentum of the elliptic point), with Λ_e solution of the equation $\Lambda_e^3 - \Delta\Lambda_e - 1 = 0$. At the same time, $\langle \sin q \rangle$ goes to -1 , which corresponds to the phase value $-\pi/2$ of the elliptic point. These behaviors are shown in Figs. 4 and 5, and represent a confirmation of the given picture of the phase-space structure.

From the above analysis, we can state that in the saturation regime, starting from the chosen initial conditions, after the lethargy the electron trajectories in phase space lie around the elliptic point, i.e., the minimum of the Hamiltonian. This can occur because of the disappearance of the hyperbolic point.

IV. PERIOD OF NONLINEAR OSCILLATIONS IN THE SATURATION REGIME

To give a more detailed insight into the behavior of the system, we refer here to the saturation regime and compute the period of the spatial nonlinear oscillations of the system using the canonical perturbation technique.

We expand the Hamiltonian function (4) in p_j around the elliptic point of coordinates $q_j = -\pi/2$ and $p_j = p_e$ ($j = 1, \dots, N$), and obtain to first order

$$H = N \frac{p_e^2}{2} + \sum_{j=1}^N \frac{x_j^2}{2} - 2\Lambda_e \sum_{j=1}^N \cos \varphi_j - \frac{1}{\Lambda_e} \sum_{j=1}^N x_j (1 - \langle \cos \varphi \rangle), \quad (15)$$

where $x_j = p_j - p_e$, and $\varphi_j = q_j + \pi/2$. The second and the third term in the right-hand side of Eq. (15) describe N identical pendulums driven by the term $2\Lambda_e$. The last term describes the coupling between the pendulums, and will be considered in the following as a perturbative term.

To describe the dynamics of the system in saturation, we look for the invariants of the system via the Lie-transformation method, and proceed as in the analysis of the nonlinear libration motion of the pendulum [10]. The Hamiltonian (15) is expanded in φ_j (around $\varphi_j = 0$), obtaining

$$H = NH_e + H_0 + H_1, \quad (16)$$

where

$$\begin{aligned} H_e &= p_e^2/2 - 2\Lambda_e, \\ H_0 &= \sum_j \left[\frac{x_j^2}{2} + 2\Lambda_e \frac{\varphi_j^2}{2} \right], \\ H_1 &= -2\Lambda_e \sum_j \left[\frac{\varphi_j^4}{4!} - \frac{\varphi_j^6}{6!} + \dots \right] \\ &\quad - \frac{1}{\Lambda_e} \frac{1}{N} \sum_{ij} x_j \left[\frac{\varphi_i^2}{2!} - \frac{\varphi_i^4}{4!} + \dots \right]. \end{aligned} \quad (17)$$

The function H_0 represents N harmonic oscillators of frequency $\omega_0 = \sqrt{2\Lambda_e}$, and H_1 contains both the nonlinear corrections of the oscillators and the coupling terms. Transforming to action angle variables of the harmonic oscillator, $\mathbf{I}, \boldsymbol{\psi}$,

$$\varphi_j = \sqrt{2I_j/\omega_0} \sin\psi_j, \quad x_j = \sqrt{2\omega_0 I_j} \cos\psi_j, \quad (18)$$

the functions H_0 and H_1 read

$$H_0(\mathbf{I}) = \omega_0 \sum_j I_j, \quad (19)$$

$$H_1(\mathbf{I}, \psi) = - \sum_j I_j^2 \sin^4\psi_j \left[\frac{1}{6} - \frac{1}{9\omega_0} I_j \sin^2\psi_j \right] \\ - \frac{2^{3/2}}{\omega_0^{5/2}} \frac{1}{N} \sum_{i,j} I_i \sqrt{I_j} \sin^2\psi_i \cos\psi_j \\ \times \left[1 - \frac{1}{6\omega_0} I_i \sin^2\psi_i \right]. \quad (20)$$

Now, following the Lie-transformation method up to second order, the Hamiltonian $H(\mathbf{I}, \psi)$ is transformed into a new Hamiltonian \bar{H} which is a function of the actions only,

$$\bar{H} = NH_e + H_0 + \langle H_1 \rangle_\psi + \frac{1}{2} \langle [w_1, H_1] \rangle_\psi. \quad (21)$$

In Eq. (21), the symbol $\langle \rangle_\psi$ denotes averaging over the angles ψ , $[w_1, H_1]$ is the Poisson bracket, and w_1 is a Lie generating function determined by the equation

$$\omega_0 \sum_{j=1}^N \frac{\partial w_1}{\partial \psi_j} = \langle H_1 \rangle_\psi - H_1. \quad (22)$$

The explicit computation of \bar{H} is rather lengthy and requires some analytical effort. In the physically relevant limit $N \gg 1$, the following simple expression is found:

$$\bar{H}(J_1, \dots, J_N) = N \left[H_e + \omega_0 \langle J \rangle - \frac{1}{16} \langle J^2 \rangle - \frac{1}{2\omega_0^6} (\langle J \rangle)^2 \right. \\ \left. - \frac{1}{256\omega_0} \langle J^3 \rangle - \frac{1}{8\omega_0^7} \langle J \rangle \langle J^2 \rangle \right]. \quad (23)$$

Here J_1, \dots, J_N are constants of the motion. In the right-hand side of Eq. (23), the third and the fifth term are the well-known terms describing the nonlinear pendulum, while the fourth and the last terms come from the coupling, and characterize the system under consideration. The expression (23) for \bar{H} is correct up to the third power of the actions. Moreover, it has been checked that the neglected terms in the Hamiltonian, coming from higher-order expansions in both the variables x_j and φ_j , give contributions to Eq. (23) which are vanishingly small in the limit $N \gg 1$.

To compute the spatial frequency of the nonlinear oscillations, we assume that due to the symmetry of the system all the actions are equal, $J_1 = \dots = J_N = \bar{J}$, and evaluate \bar{J} by the constancy of the Hamiltonian,

$$\bar{J} = \frac{1}{\omega_0} \left[\frac{\delta^2}{2} - H_e \right] = \omega_0 \left[\frac{1}{2} + \frac{\omega_0^6}{32} \right] + O(|A|_0^2). \quad (24)$$

We finally obtain the following expression for the frequency of the oscillations in the saturation regime:

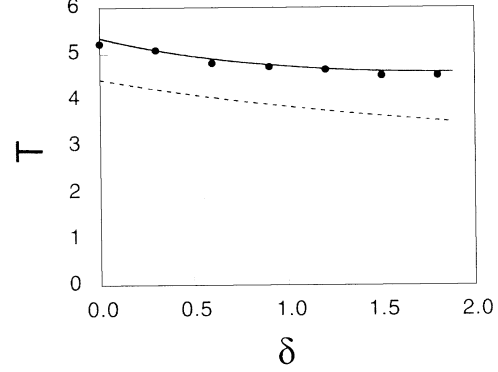


FIG. 6. Period $T = 2\pi/\bar{\omega}$ of the nonlinear spatial oscillations of the field amplitude in the saturation regime as a function of the detuning parameter δ . The solid line represents the analytical result corresponding to Eq. (25), the dots represent the numerical results obtained by direct integration of the equations of motion, and the dashed line is the period $T_0 = 2\pi/\omega_0$ of the harmonic oscillators.

$$\bar{\omega} = \frac{\partial \bar{H}}{\partial \bar{J}} = \omega_0 \left[1 - \frac{1}{8} \frac{\bar{J}}{\omega_0} - \frac{\bar{J}}{\omega_0^7} - \frac{3}{256} \frac{\bar{J}^2}{\omega_0^2} + \frac{3}{8} \frac{\bar{J}^2}{\omega_0^8} \right]. \quad (25)$$

Note that $\bar{\omega}$ is a function only of δ in the limit of negligible initial wave field excitation (i.e., for $|A|_0^2 = 0$). The comparison between the analytical expression of the frequency (25) and the numerical results obtained by direct integration of the equations of motion (7) is shown in Fig. 6. The agreement between the analytical and the numerical values is fairly good. This confirms the accuracy of our global picture of the process.

V. CONCLUSIONS

The analysis of the Compton FEL dynamics by means of an autonomous Hamiltonian with N degrees of freedom has been performed referring to an initial state characterized by a monoenergetic unbunched electron beam. It is found that the transition from small- to high-gain regime corresponds to a bifurcation in the $2N$ -dimensional phase space, where the only hyperbolic point of the system disappears.

We have shown that in the high-gain regime the dynamics is governed by the presence of a single elliptic point, which behaves as a simple attractor when dissipation is introduced in the system. In saturation, the system performs nonlinear oscillations around the elliptic point. The period of these oscillations has been computed by a canonical perturbation technique, obtaining a very good agreement with numerical simulations and substantiating the validity of our approach.

The present analysis gives insight into the nature of saturation in wave particle instabilities which can be characterized by a Hamiltonian formalism, and, besides FEL's, may be relevant to other systems such as gyrotrons, traveling-wave tubes, and beam-plasma instabilities.

ACKNOWLEDGMENT

The Istituto di Fisica del Plasma is a part of the EURATOM-ENEA-CNR Association.

- [1] L. R. Elias *et al.*, Phys. Rev. Lett. **36**, 717 (1976); D. A. G. Deacon *et al.*, *ibid.* **38**, 892 (1977).
- [2] T. J. Orzechowski *et al.*, Phys. Rev. Lett. **54**, 889 (1985).
- [3] R. Bonifacio, C. Pellegrini, and L. Narducci, Opt. Commun. **50**, 373 (1984).
- [4] C. W. Roberson and P. Sprangle, Phys. Fluids B **1**, 3 (1989).
- [5] R. Bonifacio, F. Casagrande, G. Cerchioni, L. de Salvo Souza, P. Pierini, and N. Piovella, Riv. Nuovo Cimento **13**, No. 9 (1990).
- [6] R. Bonifacio, F. Casagrande, and C. Pellegrini, Opt. Commun. **61**, 55 (1987).
- [7] R. Bonifacio, F. Casagrande, and A. Airoidi, Opt. Commun. **80**, 370 (1991).
- [8] I. A. Kotel'nikov and G. V. Stupakov, Zk. Eksp. Teor. Fiz. **84**, 956 (1983) [Sov. Phys. JETP **57**, 555 (1983)].
- [9] D. Farina and R. Pozzoli, Phys. Fluids B **3**, 1570 (1991).
- [10] A. J. Lichtenberg and M. A. Lieberman, *Regular and Stochastic Motion* (Springer-Verlag, New York, 1983).
- [11] N. M. Kroll, L. P. Morton, and M. N. Rosenbluth, IEEE J. Quantum Electron. **QE-17**, 1436 (1981).
- [12] D. Prosnitz, A. Szoke, and V. K. McNeil, Phys. Rev. A **24**, 1436 (1981).
- [13] V. I. Arnold, *Geometrical Methods in the Theory of Ordinary Differential Equations* (Springer-Verlag, New York, 1982) (Russian original, Nauka, Moscow, 1977).